Hydrodynamic interaction of particles with grafted polymer brushes and applications to rheology of colloidal dispersions

A. A. Potanin* and W. B. Russel

Department of Chemical Engineering, Princeton University, Princeton, New Jersey 08544

(Received 14 November 1994)

We calculate the lubrication force that acts in the normal direction between spherical surfaces bearing grafted polymer brushes and immersed in a viscous fluid. Brinkman's equation is employed to describe the flow in the brushes. For *noncompressed* brushes we include a slip approximation that applies to poorly permeable brushes of arbitrary density profile. For the step-function profile we present an analytical representation of the force valid for any separation. For *compressed* brushes we assume the density to increase homogeneously through the gap depending only on the local separation and derive an integral representation for the force along with analytical approximations valid up to rather strong compression. Our results generalize earlier estimates, providing convenient representations for analyses of hydrodynamic interaction between polymerically stabilized colloidal particles. As the simplest application we calculate the viscosity of a non-Brownian suspension of such particles for comparison with the measured high-shear viscosity for polymerically stabilized lattices.

PACS number(s): 36.20.−r, 81.60.Jw

I. INTRODUCTION

In recent years growing interest in the properties of grafted polymer layers (brushes) on solid-liquid surfaces has produced a considerable amount of published work dealing with the static properties of brushes (see, e.g., [1,2]) and some addressing hydrodynamic properties. Milner [3] investigated the penetration of flow into an isolated brush. Fredrickson and Pincus [4] and Kotov, Solomentsev, and Starov [5] considered the hydrodynamic interaction of particle-bearing brushes in the lubrication approximation. However, these results remain in some respects incomplete, which hinders their application to calculations of the dynamics of dispersions. Indeed, these authors confined themselves to noncompressed, $H > 2L$, and deeply compressed, $H \ll 2L$, brushes with step-function density profiles $\phi(z)$ (here H is the separation between solid surfaces, L is the height of brushes, and z is the distance from the solid surface). Only in the latter case were the hydrodynamic forces calculated analytically [4]. Several properties of grafted brushes are important, but in this paper we are primarily concerned with the viscosity of sterically stabilized dispersions as investigated recently by Mewis *et al.* [6] and Richtering [7].

Our objective is to generalize the earlier results and apply them to predict the rheology of dispersions. Let us first recall the principle equations of lubrication theory, rewriting them in a way convenient for two spherical surfaces with radius a separated by the gap $H \ll a$. Then the gap between them is locally

$$h(r) = H + \frac{r^2}{a} , \tag{1}$$

where r is the radial coordinate (see Fig. 1). In cylindrical coordinates (r,z) centered in the middle of the gap the equations for the velocity v and the pressure p are

$$\frac{1}{r}\frac{\partial}{\partial r}(rv_r) + \frac{\partial}{\partial z}v_z = 0 , \tag{2}$$

$$\frac{\partial^2}{\partial z^2}v_z + \frac{1}{r}\frac{\partial}{\partial r}r\frac{\partial v_z}{\partial r} + \frac{1}{\delta^2}v_z = \frac{1}{\mu}\frac{\partial p}{\partial z} , \tag{3}$$

$$\frac{\partial^2}{\partial z^2}v_r + \frac{1}{r}\frac{\partial}{\partial r}r\frac{\partial v_r}{\partial r} - \frac{v_r}{r^2} + \frac{1}{\delta^2}v_r = \frac{1}{\mu}\frac{\partial p}{\partial r} , \tag{4}$$

which should be solved with sticking boundary conditions on the surface of the particles and the continuity of the velocity and its derivative on the interface between
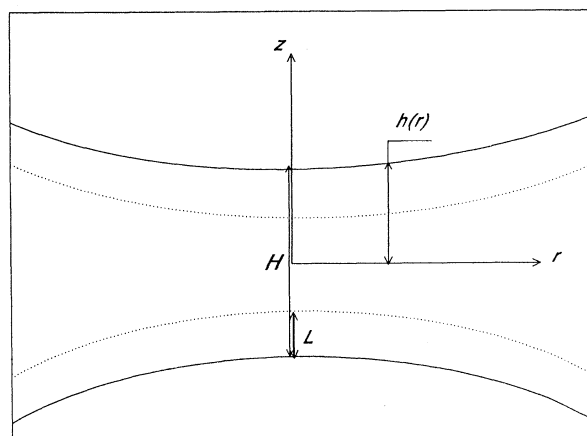

FIG. 1. Schematic of the interacting particle.

the brush and pure liquid. Here μ is the viscosity of the medium and δ^2 is the permeability, which is infinite outside the brushes where Eqs. (3) and (4) reduce to the Stokes equations and finite inside them where Eqs. (3) and (4) represent the Brinkman equations [8]. For $H \ll a$ the lubrication approximation permits Eqs. (3) and (4) to be simplified, since from Eq. (1) r scales as $(ah)^{1/2}$, while z scales as H. Hence, the second term in the left-hand side (lhs) of (4) and the second and the third terms in the lhs of (3) can be neglected relative to the first term. Then, according to (3) we write

$$\frac{p}{\mu} \sim v_r \left[\frac{1}{H} \left[\frac{a}{H} \right]^{1/2} + \frac{(1H)^{1/2}}{\delta^2} \right] , \tag{5}$$

while the two remaining terms in the lhs of (4) are negligible since

$$v_z \left[\frac{1}{H^2} + \frac{1}{\delta^2} \right] \sim v_r \left[\frac{H}{a} \right]^{1/2} \left[\frac{1}{H^2} + \frac{1}{\delta^2} \right] \ll \frac{p}{\mu H} , \tag{6}$$

with Eq. (2) relating v_z to v_r. Thus to highest order in H/a the lubrication approximation sets the lhs of Eq. (4) to zero, finally reducing the equations to

$$\frac{\partial}{\partial z} p = 0 , \tag{7}$$

$$\frac{\partial^2}{\partial z^2} v_r + \frac{1}{\delta^2} v_r = \frac{1}{\mu} \frac{\partial}{\partial r} p . \tag{8}$$

If $\delta = \mathrm{const}$, δ gives the depth that flow penetrates into the brush (see below). In general, δ is a function of the local density of polymer segments ϕ. A power law dependence is mathematically convenient,

$$\delta = \delta_1 \frac{1}{\phi^n} \equiv \delta_0 \left[\frac{\phi_0}{\phi} \right]^n , \tag{9}$$

and describes a dilute porous medium with $n = \frac{1}{2}$ and δ_1 characterizing the size of the structural units (monomers). For swollen polymer brushes δ is usually identified by the characteristic "mesh size" of the polymer solution and

$$n = \frac{\nu}{3\nu - 1} , \tag{10}$$

where ν is the exponent in the relation $R_g \sim N^\nu$ between the radius of gyration of the molecule R_g and the number of segments N. Thus, $n = \frac{1}{2}$ for linear molecules ($\nu = 1$), $n = 1$ for Gaussian coils ($\nu = \frac{1}{2}$), and $n = \frac{3}{4}$ for swollen molecules in good solvent ($\nu = \frac{3}{5}$). In (9) we introduce for convenient δ_0 and ϕ_0 as values of δ and ϕ for an equivalent step-function density profile.

There are several simplifications involved in the application of the Brinkman model to the dynamics of brushes. The power law (9) neglects the finite volume of polymer segments, which becomes important as $\phi \to 1$. One can introduce a more complicated $\delta(\phi)$ (see [9] and the following discussion), but the validity of Brinkman's equation is dubious for $\phi = O(1)$, since δ becomes comparable to the monomer size. So we use Eq. (9) as the simplest approximation. Here we also confine ourselves to

the *static* problem, assuming the brush to be unperturbed by the liquid flow. This implies that the characteristic time for particle displacement is much larger than the relaxation time, $\tau \sim \mu H^2 \delta / kT$ [4] estimated as the time for a blob of size δ to diffuse a distance H.

Solving (8) determines the velocity profile in the gap, $v_r(z)$. The continuity equation then is employed to calculate the pressure distribution from which the hydrodynamic force on a particle follows as

$$F = \int T \cdot n \, d^2 r + \int \frac{\mu}{\delta^2} (v - u) d^3 r , \tag{11}$$

where T is the stress tensor, n is the vector normal to the particle surface, and u is the velocity of the particle. The first integral is over the surface of the particle, while the second is over the internal volume of the brush. The second term, however, contributes as $O(\mu a v_z)$, which can be neglected. In the first integral in (11) the second term in the normal stress $(T \cdot n)_z = -(p - p_\infty) + 2\mu(\partial v_z / \partial z)$ also contributes as $O(\mu a v_z)$, leaving for the z component of the hydrodynamic force,

$$F = 2\pi \int_0^\infty (p - p_\infty) r \, dr , \tag{12}$$

where p_∞ is the value of p outside the gap. The integral in (12) can be written in a rather simple general form by introducing the dimensionless coordinates

$$\bar{h} \equiv \frac{h}{H}, \quad \bar{z} \equiv \frac{z}{H} \tag{13}$$

and velocity

$$v(\bar{h}, \bar{z}) \equiv \frac{v_r(h, z)}{-\dfrac{H^2}{\mu} \dfrac{\partial p}{\partial r}} . \tag{14}$$

Integrating the continuity equation (2) over z from 0 to $h/2$ and employing (14), yields an equation that relates p to v as

$$p - p_\infty = \frac{\mu V a}{8 H^2} \int_{\bar{h}}^\infty \frac{d\bar{h}'}{\int_0^{\bar{h}'/2} v(\bar{h}', \bar{z}) d\bar{z}} , \tag{15}$$

where $V \equiv -dH/dt$ is the relative velocity of the particles. It is convenient to define the dimensionless pressure as

$$P(\bar{h}) \equiv \frac{2}{3} (p - p_\infty) \frac{H^2}{\mu V a} = \frac{1}{12} \int_{\bar{h}}^\infty \frac{d\bar{h}'}{Q(\bar{h}')} , \tag{16}$$

where Q is the dimensionless flux through the half-gap,

$$Q(\bar{h}') \equiv \int_0^{\bar{h}'/2} v(\bar{h}', \bar{z}) d\bar{z} . \tag{17}$$

Substituting (16) into (12) provides the integral representation for the hydrodynamic force

$$F(H) = \frac{3\pi}{2} \frac{\mu V a^2}{H} \int_1^\infty d\bar{h} \, P(\bar{h}) . \tag{18}$$

For bare particles, $v = [(\bar{h}/2)^2 - \bar{z}^2]/2$ and Eq. (18) yields

$$F(H) = \frac{3\pi}{2}\mu V \frac{a^2}{H} , \qquad (19)$$

a widely used formula sometimes attributed to Reynolds [10]. [In actual fact, Reynolds considered parallel surfaces and did not state Eq. (19), although it follows from his equations. The history of Eq. (19) is rather obscure. Deryagin argued that Taylor first wrote this equation in 1924 (see [11], p. 346). The first complete solution to the problem was given by Brenner [12] for arbitrary H/R, from which (19) follows in the small gap limit.] For the more general case rewriting Eq. (18) as

$$F(H) = \frac{3\pi}{2}\mu V \frac{a^2}{H} k(H) , \qquad (20)$$

defines the factor

$$k(H) \equiv \int_1^\infty P(\bar{h}) d\bar{h} , \qquad (21)$$

e.g., to account for the additional force due to brushes. Now the problem is reduced to deriving the radial velocity v from which $k(H)$ follows through the triple integration in (17), (16), and (21).

In Sec. II we will consider a step-function density profile for noncompressed (and nonoverlapping) brushes, extracting an exact solution of Brinkman's equation and an analytic form for $k(H)$. In Sec. III we will turn to noncompressed brushes with "smooth" density profiles (e.g., parabolic) and estimate $k(H)$ within the framework of a slip-approximation valid for slightly permeable brushes. In Sec. IV we analyze compressed brushes assuming the local density to be independent of radial position and dependent only on the local separation, and extract an integral representation for the force along with some analytical approximations valid up to rather strong compression. Finally, in Sec. V we employ our results to calculate the viscosity of a suspension of spheres with grafted polymer brushes and demonstrate good agreement with the high-shear viscosity measured for polymerically stabilized lattices.

II. NONCOMPRESSED BRUSHES WITH THE STEP-FUNCTION DENSITY PROFILE

Let us consider the step-function density profile with $\phi = \phi_0$ and $\delta = \delta_0$ inside the brushes for separations $H > 2L$. For simplicity of notation, from here onward we write all equations for the upper brush, i.e., $z > 0$. Thus, the solution of Brinkman's equation yields

$$v\left[\bar{h}, \bar{z} < \frac{\bar{h}}{2} - \frac{L}{H}\right] = -\frac{\bar{z}^2}{2} + C \qquad (22)$$

outside the brush and

$$v\left[\bar{h}, \bar{z} > \frac{\bar{h}}{2} - \Delta\right] = \frac{1}{K^2} + B_1 e^{-K\bar{z}} + B_2 e^{K\bar{z}} \qquad (23)$$

inside it, where $K \equiv H/\delta_0$, $\Delta \equiv L/\delta_0$. The constants in Eqs. (22) and (23) follow from joining these solutions and their derivatives at the brush interface and requiring no slip at the particle surface:

$$B_1 = \frac{1}{K^2}\frac{\eta e^{-\Delta} - e^{-2\Delta}}{1 + e^{-2\Delta}} e^{\eta + \Delta} , \qquad (24)$$

$$B_2 = -\frac{1}{K^2}\frac{\eta e^{-\Delta} + 1}{1 + e^{-2\Delta}} e^{-\eta - \Delta} , \qquad (25)$$

$$C = \frac{\bar{h}_L^2}{8} + \frac{1}{K^2} - B_1 e^{-\eta - \Delta} - B_2 e^{\eta + \Delta} , \qquad (26)$$

where

$$\bar{h}_L \equiv \frac{h - 2L}{H}, \quad \eta \equiv \frac{h - 2L}{2\delta_0} . \qquad (27)$$

Now the flux follows as

$$Q(\bar{h}) = \frac{1}{3K^3}(\eta^3 + 3\eta^2 s_0 + 6\eta s_1 + s_2) , \qquad (28)$$

where

$$s_0 \equiv \tanh(\Delta), \quad s_1 \equiv \frac{(1 - e^\Delta)^2}{1 + e^{2\Delta}}, \quad s_2 \equiv 3(\Delta - s_0) . \qquad (29)$$

Making use of (17), (21), and (28), we find

$$k(H) \equiv \frac{K(s - \xi)}{2\xi^2 - r}\ln\frac{s - \xi}{(s^2 + \xi s - r)^{1/2}}$$
$$+ K\frac{d + 3\xi(2s + \xi)}{2(2\xi^2 - r)\sqrt{d}}\left[\frac{\pi}{2} - \arctan\frac{2s + \xi}{\sqrt{d}}\right] , \qquad (30)$$

where

$$s \equiv \frac{K}{2} - \Delta + s_0,$$

$$\xi \equiv -c_1^{1/3}[(\tfrac{1}{2} + \sqrt{D})^{1/3} + (\tfrac{1}{2} - \sqrt{D})^{1/3}] , \qquad (31)$$

$$D \equiv \frac{1}{4} - \frac{c_2^3}{27c_1^2}, \quad c_1 \equiv 2s_0^3 - 6s_0 s_1 + s_2 ,$$

$$c_2 \equiv 3s_0^2 - 6s_1, \quad d \equiv -\xi^2 - 4r, \quad r \equiv c_1/\xi . \qquad (32)$$

Eqs. (30)–(32) are general, although the definitions of parameters s_0, s_1, s_3 depend on the assumptions employed in calculating the flux Q. Equations (29) pertain to the step-function density profile, which permits the exact calculations as presented in this section.

For other profiles complete analyses of the intrabrush flow can be rather involved, except for poorly permeable brushes. Then, as noted by Milner [3], one can estimate the penetration length α of the liquid flow into the brush and collapse the mechanics of this region into a boundary condition as

$$\frac{v - v_\infty}{\alpha} = -\frac{\partial v}{\partial z} \quad \text{at } z = h - L , \qquad (33)$$

where v_∞ is the pressure-driven flow deep inside the brush. For very poorly permeable brush with $v_\infty \approx 0$, (33) becomes the slip boundary condition for a solid sphere, for which solution of the lubrication problem yields [13]

$$k(H) = \frac{H}{3\alpha}\left[\left[1 + \frac{H - 2L}{6\alpha}\right]\ln\left[1 + \frac{6\alpha}{H - 2L}\right] - 1\right] . \qquad (34)$$

This follows from Eqs. (17), (21), and (28) if one sets $\alpha = s_0\delta_0$, $s_1 = s_2 = 0$, thus completely neglecting intra-brush flow. Equation (34) predicts a certain weakening of the hydrodynamic force, but does not eliminate the divergence at $H = 2L$. In the next section we adapt the slip approximation by properly accounting for intrabrush flow for poorly permeable brushes, which removes the divergence.

III. SLIP APPROXIMATION FOR NONCOMPRESSED POORLY PERMEABLE BRUSHES WITH PARABOLIC DENSITY PROFILE

In this section we consider the brushes with parabolic density profile as predicted by Milner, Witten, and Cates [1]:

$$\frac{\phi}{\phi_0} = \frac{3}{2}\left[1 - \left[1 - \frac{z_L}{L}\right]^2\right] = 3\frac{z_L}{L}\left[1 - \frac{z_L}{2L}\right] , \quad (35)$$

where $z_L \equiv z - (h_L/2)$ is the distance from the brush-liquid interface, and the numerical coefficient has been chosen in such a way that the averaged density is identical to ϕ_0. Since the liquid velocity close to the interface

of the poorly permeable brush scales with the penetration length α, it is convenient to rewrite the Brinkman equation (8) inside the brush in the following form:

$$\frac{\partial^2 v}{\partial \xi^2} - \xi^{2n}\left[1 - \frac{\xi}{2\xi_0}\right]^{2n} v = -\left[\frac{\alpha}{H}\right]^2 , \quad (36)$$

where

$$\xi \equiv \frac{z_L}{\alpha}, \quad \xi_0 \equiv \frac{L}{\alpha}, \quad \alpha \equiv 3^{-n/(1+n)}(\delta_0 L^n)^{1/(1+n)} . \quad (37)$$

The redefined penetration length α turns out to be much larger than the value δ_0 for the step-function profile. An analytical solution of (36) is possible for $\xi \ll \xi_0$, where (36) reduces to

$$\frac{\partial^2 v_{\text{surf}}}{\partial \xi^2} - \xi^{2n}v_{\text{surf}} = -\left[\frac{\alpha}{H}\right]^2 \quad (38)$$

and v_{surf} distinguishes the solution from the complete v. Now we solve (38), join it with the solution (22) outside the brush, and apply the boundary condition $v_{\text{surf}}(\xi = \infty) = 0$, implying negligible flow deep in the layer. We find

$$v_{\text{surf}}\left[\bar{h}, \bar{z} > \frac{\bar{h}}{2} - \Delta\right] = v_0\frac{1}{\pi}\Gamma(1-p)p^p\sin(\pi p)K_p\left[2p\xi\frac{1}{2p}\right]$$

$$+ (2p)^{2-3p}\left[\frac{\alpha}{H}\right]^2\xi^{1/2}\left\{I_p\left[2p\xi\frac{1}{2p}\right]\int_{2p\xi(1/2p)}^{\infty}\omega^{3p-1}K_p(\omega)d\omega\right.$$

$$\left. + K_p\left[2p\xi\frac{1}{2p}\right]\int_0^{2p\xi(1/2p)}\omega^{3p-1}I_p(\omega)d\omega\right\} , \quad (39)$$

where $p \equiv 1/(2n+2)$ and v_0 is the liquid velocity at the interface:

$$v_0 \equiv \frac{\Gamma(1-p)}{2p^{2p}\Gamma(1+p)}\frac{\alpha h_L}{H} + \frac{\Gamma(2p)\Gamma(p)\Gamma(1-p)}{p^p[\Gamma(1+p)]^2}\left[\frac{\alpha}{H}\right]^2 . \quad (40)$$

Outside, the brush (22) takes the form

$$v\left[\bar{h}, \bar{z} < \frac{\bar{h}}{2} - \bar{\Delta}\right] = -\frac{\bar{z}}{2} + \frac{\bar{h}_L^2}{8} + v_0 . \quad (41)$$

The asymptotic representation v_{surf}^{∞} for v_{surf} follows from (39) as

$$v(\xi_0 \gg \xi \gg 1) = v_{\text{surf}}(\xi \gg 1) = v_{\text{surf}}^{\infty}(\xi)$$

$$\equiv \left[\frac{\alpha}{H}\right]^2\xi^{-2n} , \quad (42)$$

while the correct asymptotic solution deep inside the brush, easily seen from (36), is

$$v(\xi_0 > \xi \gg 1) = v^{\infty}(\xi) \equiv \left[\frac{\alpha}{H}\right]^2\xi^{-2n}\left[1 - \frac{\xi}{2\xi_0}\right]^{-2n} . \quad (43)$$

Both Eqs. (42) and (43) correspond to the Darcy approximation for the Brinkman equation but the density profile is assumed linear in (42), as opposed to the full parabolic profile in (43).

Let us write the liquid velocity in the brush as

$$v(\xi) = v_{\text{surf}}(\xi) + \Delta v(\xi) , \quad (44)$$

where $\Delta v(\xi)$ is the difference between the solutions of (36) and (38). The corresponding representation for the flux

$$Q = Q_{\text{out}} + Q_{\text{surf}} + \Delta Q , \quad (45)$$

with

$$Q_{\text{out}} = \int_0^{\bar{h}_L/2} v\,d\bar{z} = \frac{\bar{h}_L^3}{24} + \frac{\bar{h}_L v_0}{2} , \quad (46)$$

$$Q_{\text{surf}} = \frac{\alpha}{H}\int_0^{\xi_0} v_{\text{surf}}d\xi , \quad (47)$$

includes contributions from the flow (41) outside the brush and (39) within it plus

$$\Delta Q = \frac{\alpha}{H}\int_0^{\xi_0}\Delta v\,d\xi , \quad (48)$$

the correction that arises from approximating v by v_{surf}.

Now we will express the solution in a compact form valid for $\frac{1}{2} < n < 1$. The first inequality guarantees that the upper limit of the integral in (47) can be set to infinity, i.e., the dominant contribution to this integral comes from the surface layer of the brush (see below). The second inequality permits us to substitute into (48) the difference between asymptotes $v^{\infty} - v_{\mathrm{surf}}^{\infty}$ instead of the difference between complete solutions $v - v_{\mathrm{surf}}$. This procedure is justified if the dominant contribution to (48) is the deeply penetrating Darcy flow at $\xi = O(\xi_0)$ rather than the flow in the viscous surface layer at $\xi \ll \xi_0$. Expanding $v^{\infty} - v_{\mathrm{surf}}^{\infty}$ at $\xi \ll \xi_0$, one finds

$$
v^{\infty} - v_{\mathrm{surf}}^{\infty} = \left[\frac{\alpha}{H} \right]^2 \xi^{-2n_0} \left[n \left[\frac{\xi}{\xi_0} \right]^{1-2n} \right.
$$
$$
+ \frac{n(1+2n)}{4} \left[\frac{\xi}{\xi_0} \right]^{2-2n}
$$
$$
\left. + \cdots \right] . \tag{49}
$$

Substituting into (48) is justified for $n < 1$ since (48) reduces to

$$
\Delta Q = \frac{\alpha}{H} \int_0^{\xi_0} (v^{\infty} - v_{\mathrm{surf}}^{\infty}) d\xi = C_{\infty} \left[\frac{\alpha}{H} \right]^3 \xi_0^{1-2n} , \tag{50}
$$

with the numerical coefficient

$$
C_{\infty} \equiv \int_0^1 \left[\left[1 - \frac{\varepsilon}{2} \right]^{-2n} - 1 \right] \frac{d\varepsilon}{\varepsilon^{2n}} . \tag{51}
$$

The formula for the flux follows as

$$
Q = \frac{1}{24} \bar{h}_L^3 + \frac{1}{4} C_0 \frac{\alpha}{H} \bar{h}_L^2 + C_1 \left[\frac{\alpha}{H} \right]^2 \bar{h}_L + \frac{1}{3} C_2 \left[\frac{\alpha}{H} \right]^3 , \tag{52}
$$

with

$$
C_0 \equiv \frac{\Gamma(1-p)}{p^{2p} \Gamma(1+p)} , \tag{53}
$$

$$
C_1 \equiv \frac{\Gamma(2p)\Gamma(p)\Gamma(1-p)}{2p^{2p}[\Gamma(1+p)]^2}
$$
$$
\times \left\{ p^p + \frac{2^{p-1}}{\pi} \sin(\pi p)\Gamma(1-p)\Gamma(1+p) \right\} , \tag{54}
$$

$$
C_2 \equiv \left[\frac{2}{p} \right]^p \frac{3 \sin(\pi p)}{2\pi} \left\{ \frac{\Gamma(2p)\Gamma(p)\Gamma(1-p)}{\Gamma(1+p)} \right\}^2
$$
$$
+ 3 \left[J + C_{\infty} \left[\frac{\alpha}{L} \right]^{2n-1} \right] , \tag{55}
$$

$$
J \equiv \int_0^{\infty} d\omega \int_{\omega}^{\infty} d\omega' (\omega \omega')^{3p-1} I_p(\omega) K_p(\omega') . \tag{56}
$$

The latter integral converges for $n > \frac{1}{2}$. The contribution of the deeply penetrating Darcy flow, represented by the second term in the square brackets in (55) is small in the limit $\alpha \ll L$. The flux Q can be written in the form of (28) with

$$
s_0 \equiv C_0 \alpha / \delta_0, \quad s_1 \equiv C_1 (\alpha / \delta_0)^2, \quad s_2 \equiv C_2 (\alpha / \delta_0)^3 . \tag{57}
$$

Equations (30)–(32) still apply, with (57) substituting for (29).

Thus, in this section we have derived estimates for the lubrication force valid for poorly permeable brushes ($\delta_0 \ll L$) with a parabolic density profile and $\frac{1}{2} < n < 1$. Hence, our results apply to the most important case of swollen brushes in good solvent with $n = \frac{3}{4}$ [see the text below Eq. (10)]. The validity of our approximation also depends on the applicability of the Brinkman equation at the length scale α. Recall that our model implies that the brush is spatially homogeneous, which holds for $\phi > \phi^* \sim N^{1-3\nu}$ [14]. Estimating ϕ at $z_L \sim \alpha \ll L$ by (35) and setting $L \sim R_g \sim N^{\nu}$ converts this inequality into

$$
N^{(1-3\nu)\nu/(4\nu-1)} \gg N^{1-3\nu} , \tag{58}
$$

which is satisfied at least for $N \gg 1$ and $\nu > \frac{1}{3}$, i.e., our calculations are indeed justified.

IV. COMPRESSED BRUSHES

At $h < 2L$ the brushes come into contact, which results in either compression or interpenetration. One can show that in the mean field approximation for good solvents interpenetration produces lower free energy only below a particular separation [2]. A constant density of polymer segments between solid surfaces, i.e.,

$$
\frac{\phi}{\phi_0} = \frac{2L}{h}, \quad \delta_r \equiv \frac{\delta}{\delta_0} = \left[\frac{h}{2L} \right]^n \tag{59}
$$

is confirmed by computer simulations of interacting brushes in good solvent [15].

The velocity profile in compressed brushes at $h < 2L$ follows from (8) as

$$
v(h < 2L) = \left[\frac{\delta}{H} \right]^2 \left[1 - \frac{\cosh \left[\dfrac{z}{\delta} \right]}{\cosh \left[\dfrac{h}{2\delta} \right]} \right] . \tag{60}
$$

Combining (60) with the solution outside the compression area [which is still given by Eqs. (22) and (23) or (39) and (40)], we subsequently calculate the integrals in (17), (16), and (21). Since the integral in (16) is calculated from h to infinity, it is convenient to separate the part arising from outside the compression zone ($h' \geq 2L$) and the one from the compression zone ($2L > h' > h$). The former is identical to $P(h = 2L)$ for noncompressed brushes and hence follows from the results in Secs. II and III. The latter requires integration of (60), which yields

$$
P(h < 2L) = P(h = 2L) + \frac{K^2}{6} \int_{h/2\delta_0}^{L/\delta_0} \frac{1}{\delta_r^3} \frac{d\eta}{\dfrac{\eta}{\delta_r} - \tanh \left[\dfrac{\eta}{\delta_r} \right]} . \tag{61}
$$

Integrating (61) with (59) and substituting into (23) deter-

mines $k(H)$. Again we distinguish the portion of (23) from the noncompressed zone, which equals $k_0 = k(H = 2L)$ calculated for noncompressed brushes in Secs. II and III. We also distinguish the part that comes from integration of the first term in (61) over $H < h < 2L$, which we denote $k_1(H)$. The remaining part, $k_2(H)$, involves exclusively the integration over compressed zone. For a strongly compressed brush, $H \ll L$, $k \approx k_2$, as assumed in the earlier work of Fredrickson and Pincus [4]. Here we obtain a more general result:

$$k(H) = k_0(H) + k_1(H) + k_2(H) ,$$ (62)

where

$$k_1(H) \equiv \frac{K \left[\frac{K}{2} \Delta \right]}{2\xi^2 - r} \left[\ln \frac{s_0 - \xi}{[s_0^2 + \xi s_0 - r]^{1/2}} + \frac{3\xi}{\sqrt{d}} \left[\frac{\pi}{2} - \arctan \frac{2s_0 + \xi}{\sqrt{d}} \right] \right] ,$$ (63)

$$k_2(H) \equiv \frac{K}{3(1-n)} \int_{K/2}^{\Delta} d\eta \int_{\Delta^n \eta^{1-n}}^{\Delta} d\eta' \left[\frac{\Delta}{\eta'} \right]^{2n/(1-n)} \times \frac{1}{\eta' - \tanh(\eta')} ,$$ (64)

for $n \neq 1$, and

$$k_2(H) \equiv \frac{1}{3} \frac{\Delta^3}{\Delta - \tanh(\Delta)} \left[1 - \frac{K}{\Delta} + \left[\frac{K}{2\Delta} \right]^2 \right]$$ (65)

for $n = 1$. One can see that only for $n = 1$ are all integrals calculated analytically. However, some useful analytical approximations apply more generally.

Let us consider poorly permeable brushes, $\Delta \gg 1$, with weak compression, $\Delta^n K^{1-n} \gg 1$ (e.g., $K \gg 1/\Delta^3$ for $n = \frac{3}{4}$), such that $\tanh(\eta)$ in the denominator of (64) can be neglected, leading to

$$k_2(H) = \frac{1}{6n} K \left\{ \frac{\Delta}{2n-1} \left[\left[\frac{2\Delta}{K} \right]^{2n-1} - 1 \right] + \frac{K}{2} - \Delta \right\}$$ (66)

for $n \neq \frac{1}{2}$, $n \neq 1$;

$$k_2(H) = \frac{1}{3} K \Delta \left[\ln \frac{2\Delta}{K} + \frac{K}{2\Delta} - 1 \right]$$ (67)

for $n = \frac{1}{2}$. For $K \ll \Delta$, Eqs. (66) and (67) simplify further; e.g., (66) reduces to

$$k_2(H) = \frac{\Delta^{2n} \left[\frac{K}{2} \right]^{2(1-n)}}{3n(2n-1)} .$$ (68)

Comparing this with (34) we conclude that, at $K \gg \Delta^{(1-3n)/3(1-n)}$, k_2 provides a dominant contribution to k. Thus, Eq. (68) comprises a simple estimate for k
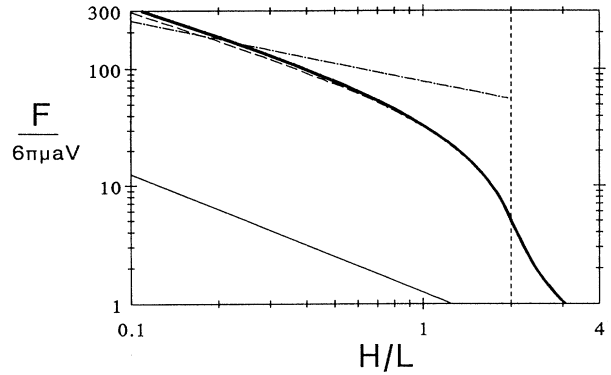

FIG. 2. Force is plotted vs gap width for step-function density profile. The thick curve represents the complete solution. Also shown are the approximations (67) (— — —) and (68) (—·—). The thin solid line corresponds to bare particles. The dashed vertical line represents the point of contact of the brushes $\Delta = 10$; $n = \frac{3}{4}$; $a/L = 5$.

and, for $n = \frac{3}{4}$, reduces to that of Fredrickson and Pincus [4], $k \sim \Delta^{3/2} K^{1/2}$. However, the applicability of this estimate is limited, e.g., to $\Delta \gg K \gg 1/\Delta^{5/3}$ for $n = \frac{3}{4}$, according to the conditions mentioned above.

Now let us consider the predictions from Eqs. (62)–(68). First we assume noncompressed brushes to have a step-function profile and employ Eqs. (31)–(34) for $k(H)$, etc. Results of calculations with $n = \frac{3}{4}$, $a = 5L$, and $\Delta = 10,100$ are plotted in Figs. 2 and 3, along with approximate solutions according to Eqs. (67) and (68). While the former approximation turns out to be very good over practically the whole range of gap widths, the latter is valid only at high Δ and very small gap width. The failure of the Fredrickson and Pincus approximation (68) at low compression is essential to the rheological problem considered in the next section. In Fig. 4 we compare solutions with different n for the step-function profile. One can see that the curves deviate from each other as the brushes become compressed, with hydrodynamic resistance increasing with n.

For a parabolic profile the slip approximation for $\Delta = 10$ and 100 is shown in Fig. 5, along with the complete solution for the step-function profile with the same
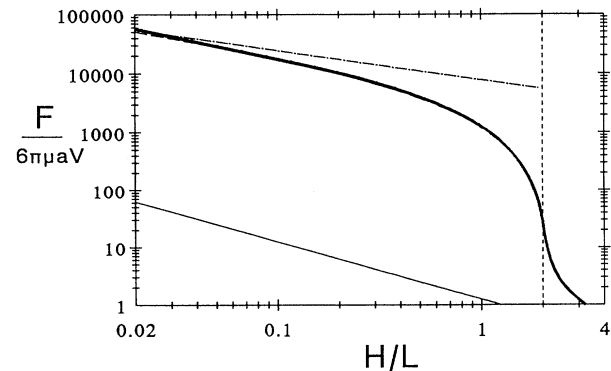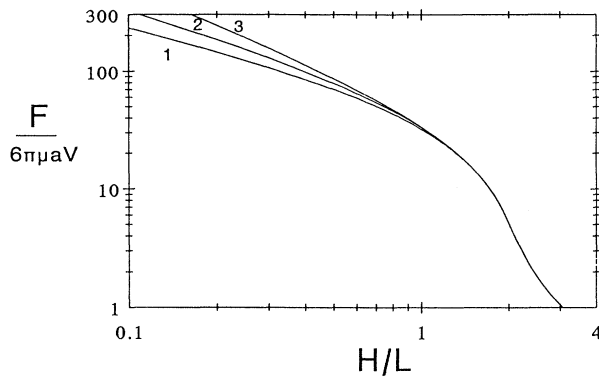

FIG. 3. Same as in Fig. 2, but for $\Delta = 100$.

FIG. 4. Force is plotted vs gap width for $\Delta = 10$ and $n = \frac{1}{2}(1)$, $\frac{3}{4}(2)$, and $1(3)$.

L. One can see that the hydrodynamic resistance is somewhat lower for a parabolic profile of the same thickness and the same average density, especially near the point of contact ($H = 2L$).

V. APPLICATION: VISCOSITY OF COLLOIDAL DISPERSION

In this section we consider a colloidal dispersion stabilized by grafting polymer chains to the surfaces of particles. Without brushes this system reduces to the hard spheres (HS) studied widely in recent decades. Of the two principal contributions to the stress tensor, hydrodynamic and thermodynamic, we address the former, which determines the high-frequency viscosity η'_∞ and the high shear viscosity η_∞. These two limits differ since steady shear perturbs the structure, substantially making the high shear viscosity somewhat higher than the high-frequency one (see, e.g., [16]). In this paper, however, we neglect this difference as insignificant compared to the effects of the brushes on the viscosity considered below.

Earlier Frankel and Acrivos [17] noted that at high volume fractions of particles ϕ close to the random packing limit ϕ_m, the hydrodynamic contribution to the
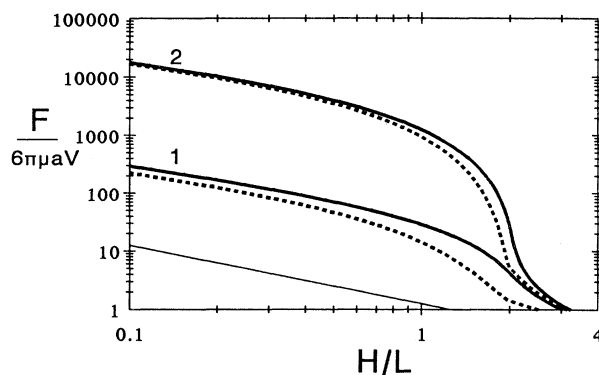
viscosity is dominated by lubrication forces. By calculating the dissipation due to lubrication in a specific configuration of particles subjected to elongation flow, they derived

$$\frac{\eta_\infty}{\mu} = \frac{3}{4\pi} \frac{F(H_{av})}{\mu V a} = \frac{9}{4} \frac{a}{H_{av}} \ , \tag{69}$$

with the lubrication force $F(H_{av})$ estimated via Eq. (19) by setting H equal to the average value H_{av} related to the volume fraction as

$$\frac{H_{av}}{2a} = \left[\frac{\phi_m}{\phi} \right]^{1/3} - 1 \ . \tag{70}$$

Many authors criticized the derivation of Eq. (69) proposed by Frankel and Acrivos (e.g., [18,19]), although certainly lubrication forces dominate at high concentrations for HS. Indeed, Frankel and Acrivos found that Eq. (69) agrees well with considerable experimental data at $0.55 > \phi > 0.20$ with $\phi_m = 0.60 \pm 0.03$.

Several efforts have sought a correspondence between the HS and the dispersion of particles with grafted brushes (see [6,20]). Obviously, there are two extreme assumptions: either to incorporate the brushes into the hard core and redefine the volume fraction as $\phi_{eff} = \phi(a + L)^3/a^3$ or to neglect totally the brushes. For the high shear viscosity at high ϕ neither assumption works, with the true value of the viscosity lying between the two extremes. Now we will solve the problem by accounting for the hydrodynamic interaction of brushes via the approach developed in this paper.

To generalize Eq. (69) for particles with brushes, we simply substitute into (69) Eq. (20) instead of Eq. (19), which gives

$$\frac{\eta_\infty}{\mu} = \frac{9}{4} \frac{a}{H_{av}} k(H_{av}) \ . \tag{71}$$

Figure 6 compares calculations from (71) with the experi-

FIG. 5. Force is plotted vs gap width for step-function (solid thick curves) and parabolic (dashed curves) density profiles for $n = \frac{3}{4}$, $a/L = 5$, $\Delta = 10(1)$, and $\Delta = 100(2)$. The thin solid line corresponds to bare particles.
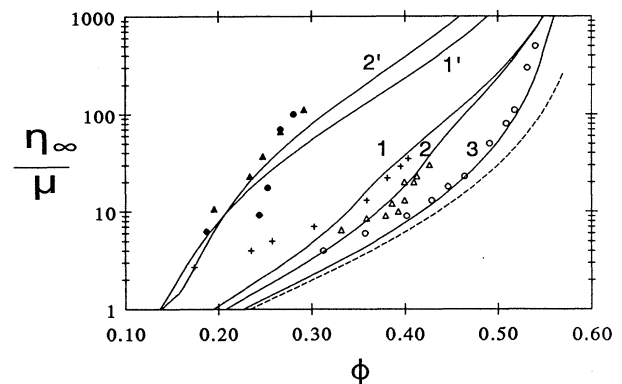

FIG. 6. Relative high-shear viscosity is plotted as a function of volume fraction for PMMA and PS systems. Calculations (curves) and experiments (points) correspond to the following a/L. For PMMA, 4.7 (1,+), 7.2 (2,△), 26 (3,○); for PS, 1.52(l',▲), 1.75 ($2'$,●). See text for other parameters. The dashed curve corresponds to HS ($k = 1$).

mental data for several different polymerically stabilized dispersions. Mewis and co-workers [6,21] dispersed in decalin poly(methyl methacrylate) (PMMA) particles stabilized by grafted poly(hydroxystearic acid). The thickness of the polymer brushes was approximately $L = 9$ nm and the particles' diameters were $2a = 84$, 129, and 475 nm (i.e., $a/L = 4.7$, 7.2, and 26). The recent data of Richtering [7] for polysterene (PS) particles with grafted poly(vinyl alcohol) involved considerably thicker brushes with $L = 100$ and 74 nm and particles with $2a = 350$ and 226 nm (thus $a/L = 1.75$ and 1.52). In all these systems the particles were highly monodispersed and spherical and layer thicknesses were determined from dilute viscometry measurements via Einstein's equation $\eta_\infty = (1 + 2.5\phi_{\text{eff}})\mu$. For the rather thin polymer layers of Mewis *et al.* one must be wary about applying the mean or self-consistent field theories cited above. However, assuming these "brushes" to have step-function profiles with a permeability $\delta_0 = 2$ nm, about twice the segment length for this type of a polymer [2], produces respectable agreement with the data for all three systems at high ϕ. The fact that the theory underestimates η_∞ at low ϕ is not surprising since lubrication forces rapidly decay at high separations, while long-range interactions are not taken into account in this model. For the PS particles we assumed a parabolic density profile and employed the slip approximation to calculate $k(H_{\text{av}})$ with $\delta_0 = 5$ nm. In all calculations we assumed $n = \frac{3}{4}$. All the data and calculation results are plotted in Fig. 6.

An important feature of the $\eta_\infty(\phi)$ curves is that they have inflection points (second derivative changes sign), which is associated with similar inflection points in $F(H)$ curves (see Fig. 5). The origin of such behavior is that the hydrodynamic resistance strongly increases as the brushes approach each other. Quantitatively this behavior can be seen in the experiments of Richtering.

Thus, in our model the agreement with the experimental data is achieved by adjusting the only parameter, δ_0. Unfortunately, experimental data on δ_0 in polymer solutions are scarce. The only measurements of which we are aware are those of Richter *et al.* [22], who found the hydrodynamic screening length for poly(dimethylsiloxane) dissolved in deuterated chlorobenzene to decrease from 2 to 0.5 nm as the polymer concentration increased from 0.15% to 0.5%, with the exponent n somewhere between $\frac{3}{4}$ and 1. In light of these data our choice of δ_0 seems reasonable.

VI. CONCLUSION

We have extended the earlier treatment [4,5] of the lubrication forces between polymer brushes on solid spherical surfaces. For the step-function density profile we obtained a representation for the lubrication force F valid at arbitrary gap width H both for noncompressed and compressed brushes. For the parabolic density profile we include an approximate analysis of poorly permeable brushes. We employ our calculations of the lubrication force to estimate the viscosity of the colloidal dispersions with grafted polymer brushes, in agreement with the experimental data for several different sterically stabilized colloidal dispersions.

ACKNOWLEDGMENTS

[1] S. T. Milner, T. A. Witten, and M. E. Cates, Macromolecules **21**, 2610 (1988).

[2] W. B. Russel, D. A. Saville, and W. R. Schowalter, *Colloidal Dispersions* (Cambridge University Press, Cambridge, 1989), Chap. 6.

[3] S. T. Milner, Macromolecules **24**, 3704 (1991).

[4] G. H. Fredrickson and P. Pincus, Langmuir **7**, 786 (1991).

[5] A. A. Kotov, Yu. E. Solomentsev, and V. M. Starov, Colloid J. USSR **53**, 867 (1991).

[6] J. Mewis, W. J. Frith, T. A. Strivens, and W. B. Russel, AIChE J. **35**, 415 (1989).

[7] S. Neuhäusler and W. Richtering, Colloids Surf. **97**, 39 (1995).

[8] H. C. Brinkman, Appl. Sci. Res. A **1**, 27 (1947).

[9] J. Klein, Colloids Surf. **86**, 63 (1994).

[10] O. Reynolds, Philos. Trans. R. Soc. London **157**, 177 (1886).

[11] B. V. Deryagin, N. A. Krotova, and V. P. Smilga, *Adhesion of Solids* (Consultants Bureau, New York, 1978), p. 346.

[12] H. Brenner, Chem. Eng. Sci. **16**, 242 (1961).

[13] A. A. Potanin, N. B. Uriev, and V. M. Muller, Colloid J. USSR **50**, 429 (1988).

[14] P.-G. de Gennes, *Scaling Concepts in Polymer Physics* (Cornell University Press, Ithaca, 1979).

[15] R. Toral, A. Chakrabarti, and R. Dickman, Phys. Rev. E **50**, 343 (1994).

[16] W. B. Russel and P. R. Sperry, Prog. Org. Coatings **23**, 305 (1994).

[17] N. A. Frankel and A. Acrivos, Chem. Eng. Sci. **22**, 847 (1967).

[18] G. K. Batchelor, Annu. Rev. Fluid Mech. **6**, 227 (1974).

[19] G. Marrucci and M. M. Denn, Rheol. Acta **24**, 317 (1985).

[20] U. Genz, B. D'Arguanno, J. Mewis, and R. Klein, Langmuir **10**, 2206 (1994).

[21] J. Mewis and P. D'Haene, Katholieke Universiteit te Leuven, Report No. ARR06-07, 1989 (unpublished).

[22] D. Richter, K. Binder, B. Ewen, and B. Stuhn, J. Phys. Chem. **88**, 6618 (1984).